Dalton Transactions

Accepted Manuscript

This article can be cited before page numbers have been issued, to do this please use: Y. Kalinovskyy, N. J. Cooper, M. Main, S. J. Holder and B. A. Blight, *Dalton Trans.*, 2017, DOI: 10.1039/C7DT03616G.

ROYAL SOCIETY OF CHEMISTRY

rsc.li/dalton

View Article Online
DOI: 10.1039/C7DT03616G

Dalton Transactions

ARTICLE

Microwave-Assisted Activation and Modulator Removal in Zirconium MOFs for Buffer-Free CWA Hydrolysis†

Received 00th January 20xx,
Accepted 00th January 20xx

DOI: 10.1039/x0xx00000x

www.rsc.org/

Y. Kalinovskyy[a], N. J. Cooper[b], M. J. Main[b], S. J. Holder[a] and B. A. Blight[*ac]

A novel, facile and efficient method was developed for the activation of acetic acid modulated zirconium MOFs. The protocol involves briefly heating the material in water with using microwave irradiation. MOF-808, DUT-84 and UiO-66 were all activated in this manner to remove the modulator and organic solvent from the framework post synthesis, with retention of MOF integrity post activation. The degree of activation was characterised by the use of TGA and NMR. The catalytic activity of the activated MOFs and their non-activated counterparts was investigated for chemical warfare agent (CWA) hydrolysis. Upon activation, an increase in the rate of hydrolysis was observed in the degradation of CWA simulant dimethyl 4-nitrophenyl phosphate (DMNP). MOF-808 and DUT-84 were also screened as catalysts for the hydrolysis of the V-series agent VM, with remarkable half-lives obtained for MOF-808 in the absence of any buffers. Currently employed MOF activation procedures involve the use of additional organic solvents post synthesis, we believe this method to be ideally efficaceous for the organic desolvation of zirconium MOFs and removing modulator additives.

Introduction

Zirconium Metal-organic frameworks (MOFs) are highly modular[1,2] and robust[3,4] structures which exhibit a high degree of porosity.[5,6] These properties have allowed zirconium MOFs to find uses in applications such as gas sorption,[7,8] drug delivery[9,10] and fluorescence sensing.[11,12] Additionally, the abundance of Lewis acidic Zr^{4+} sites on the Zr_6 secondary building unit (SBU) has made these frameworks an attractive material for organic catalysis.[13,14] A number of solvent free and mechanochemical[15,16] routes have been reported for zirconium MOF assembly, however, the vast majority of methods rely on hydrothermal synthesis.[17,18] These hydrothermal techniques often employ high boiling point solvents such as DMF and a monodentate acid modulator.[19,20] The modulator is essential for controlling the assembly of the structure and can readily influence the pore size, dimensionality and even the concentration of defects in the framework.[19,21] Post synthesis, additional steps are required to 'activate' the MOF. Activation can simply refer to the desolvation of the MOF pores (i.e. removal of organic reaction solvent), it can also be used to describe the extraction of any free or bound modulator used during synthesis to create vacancies.[21,22] For clarity, in this paper we will take the meaning of activation to be both of these. Zirconium MOFs are typically desolvated by the use of solvent exchange techniques where the MOF is soaked in a low boiling point organic solvent, this solvent is then exchanged a number of times before subjecting the material to a high dynamic vacuum. Modulators can be removed either by high temperatures, which can compromise the structural integrity,[23,24] or by post-synthetic exchange (PSE) for an alternative moiety.[22,25] Herein, we present a facile method for the activation of three known zirconium MOFs; DUT-84 (6-connected),[26] MOF-808 (6-connected),[27] and defective UiO-66.[21] The protocol utilises microwave irradiation and water to facilitate the removal of the acetic acid modulator from the Zr_6 SBU. Employing these MOFs with hydrated vacancies, we further demonstrate enhanced catalytic activity in the hydrolysis of selected organophosphorus compounds.

Zirconium MOFs with missing linker defects/coordination vacancies, such as MOF-808,[28,29] Nu-1000[30] and UiO-67-NH_2[31] have been shown to effectively catalyse the degradation of organophosphorus chemical warfare agents (CWAs). In the presence of *N*-ethylmorpholine buffer, dimethyl 4-nitrophenyl phosphate (DMNP; a well-established hydrolysis simulant)[32,33] closely mimics the hydrolytic breakdown of V-agents such as VX and VM.[31] We used this system to probe the degradation rates of the activated catalysts and compared them to the degradation rates of their as-synthesised counterparts. As hypothesised, a modest increase in the rate of hydrolysis was observed using the activated material. We then subsequently tested MOF-808 and DUT-84 on the V-series agent VM (diethylaminoethyl O-ethyl methylphosphono-thioate). Unlike DMNP, the screening of VM was conducted in the absence of buffer as the minimisation of additional reagents is essential for enhancing the practical application of these catalysts. Both

[a] School of Physical Sciences, University of Kent, Canterbury, CT2 7NH, UK.
[b] DSTL, Porton Down, Salisbury, SP4 0JQ, Wiltshire, UK
[c] Department of Chemistry, University of New Brunswick, Toole Hall, Fredericton, NB E3B 5A3, Canada. E-mail: b.blight@unb.ca

†Electronic Supplementary Information (ESI) available: ESI contains all experimental procedures, instrumentation details, CHN data for all materials, all exchange NMR spectra, PXRD patterns for all materials, TG data and reaction rates constants. See DOI: 10.1039/x0xx00000x

View Article Online
DOI: 10.1039/C7DT03616G

the as-synthesised and activated variants of MOF-808 were highly successful at hydrolysing VM. The activated variant of DUT-84 was also successful at hydrolysing VM, albeit at a slower rate than the MOF-808 variants.

Experimental

Material

All reagents and solvents were used without further purification. DMNP was prepared and purified using a previously reported procedure. MOF-808,[28] DUT-84,[26] and defective UiO-66[21] (Fig. 1) were all synthesised using slightly modified procedures using acetic acid to modulate each of their syntheses. (S2–S3, ESI†)

General procedure for Microwave assisted activation

A CEM Explorer Microwave Reactor with dynamic power cycling was used for all MOF activation steps. 200 mg of as synthesised MOF (nUiO-66, nDUT-84 or nMOF-808) was suspended in 7 ml of distilled water in an 11 ml microwave vessel. The vessel was sealed and placed in a microwave reactor where it was activated at 150°C for 20 minutes with heavy stirring using a automated power program to regulate the temperature at 150°C. After cooling to room temperature, the MOF was vacuum filtered, washed with H_2O 3 x 10 ml and acetone 3 x 10 ml to yield the activated material, aUiO-66, aDUT-84 or aMOF-808.

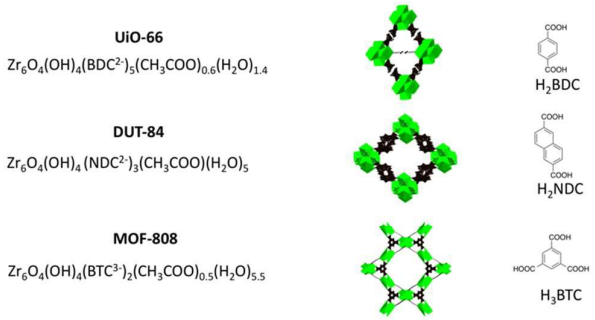

Figure 1. Formula units and graphical representations of the activated zirconium MOFs.

DMNP and VM hydrolysis procedure

The following procedure was used to probe the hydrolysis rates of the as-synthesised MOFs and their activated counterparts. An NMR tube was charged with DMNP, 20 μL (0.09 mmol). The MOF catalyst (0.11 μmol, 1.25 mol%) was then added to the tube. 0.1 ml of D_2O along with 0.5 ml of 0.1 M *N*-ethyl morpholine aqueous buffer (0.1M) was then added to the tube. The tube was inverted 3 times and immediately loaded into an NMR auto-sampler and the first spectrum was obtained within 3 minutes of the reaction commencing. The sample was then cycled on the auto-sampler to collect subsequent data points. For VM, the same procedure and the same ratios were used, the only difference was that the testing was conducted in the absence of any buffer.

Results and Discussion

Table 1. A comparison of the degree of activation achieved for each MOF based on the ratio of acetate to ligand, as observed by ^{1}H NMR

	nMOF-808	aMOF-808	nDUT-84	aDUT-84	nUiO-66	aUiO-66
Acetate:Ligand ratio	1.62	0.26	0.6	0.33	0.22	0.07
Acetate per unit	3.25	0.5	1.9	1.0	1.4	0.6
Exchange Efficiency		**84.6%**		**47.3%**		**57.1%**
Acetate removed		**2.75**		**0.9**		**0.8**
Acetate-free sites[a]		**5.5**		**5**		**1.4**

[a]The amount of coordination sites per formula unit cell that are free of modulator, this only applies to the activated counterpart of each MOF.

The degree of activation was initially investigated by digesting each of the as-synthesised MOFs (henceforth termed non-activated (n); ie. nMOF-808) and their activated (a; ie. aMOF-808) counterparts in a mixture of DMSO/D_2SO_4. Proton NMR spectra were then acquired and the ratio of ligand/acetic acid was determined for each MOF, as shown in Table 1.

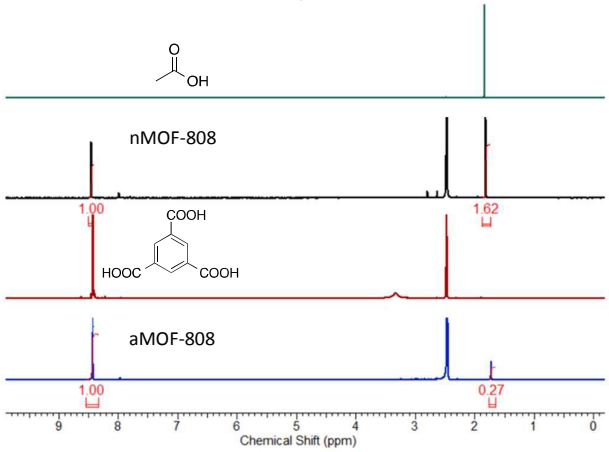

Figure 2. A ^{1}H NMR (in DMSO/D_2SO_4) overlay showing acetic acid (green), digested nMOF-808 (black), free BTC ligand (red) and the digested aMOF-808 (blue).

Partial removal of the acetate modulator was achieved for all activated MOFs. The complete extraction of residual DMF used in synthesis was also observed for all activated samples. Each Zr_6 SBU can coordinate 12 carboxylate moieties in total.

The most efficient exchange was achieved for MOF-808[28] (Fig. 2) which has a strut connectivity of 6, with 2.75 acetate ligands removed per unit, leaving 5.5 free coordination sites. DUT-84[26] also has a strut connectivity of 6, but only 0.9 acetates per formula unit were removed resulting in 5 unmodulated sites. This is because the non-activated material possesses just 2 acetate modulated sites. aUiO-66 had the lowest quantity of acetate removed per unit owing to its higher strut connectivity requiring 10 sites,[21] this meant that there were fewer available coordination vacancies for the modulator to occupy.

View Article Online
DOI: 10.1039/C7DT03616G
Dalton Transactions ARTICLE

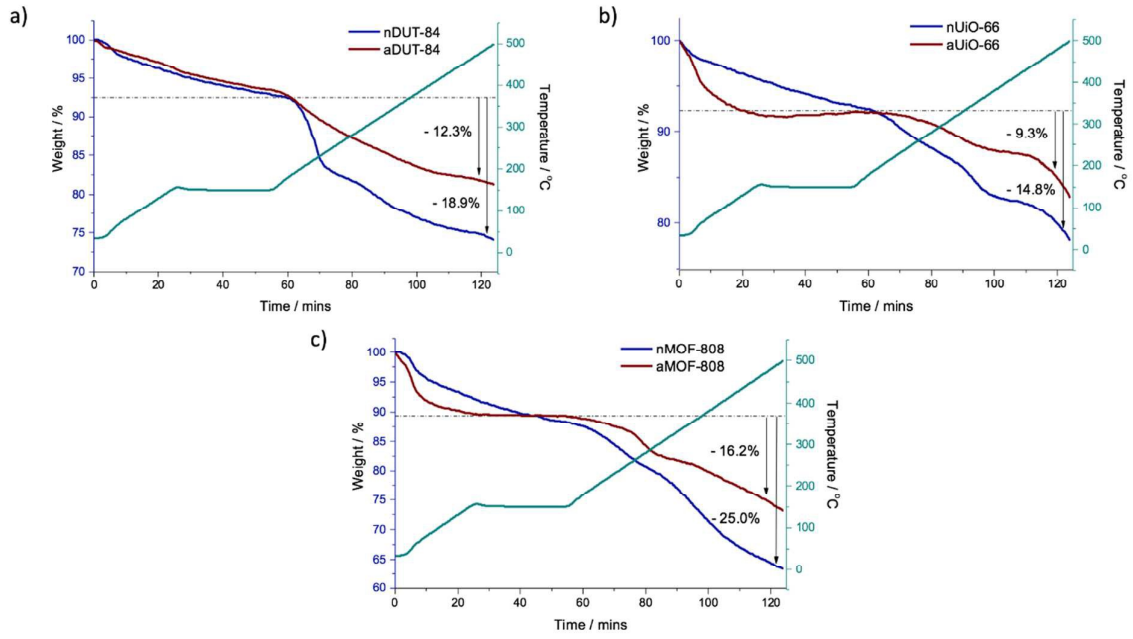

Figure 3. TGA trace for the non-activated and activated counterparts of each MOF. Heating rate: 5 °C min^{-1} in N_2, 30 min isotherm at 150°C followed by a ramp to 500°C. A value for the % weight loss post isotherm until end of the final ramp is shown on the TGA trace for each material.

The optimum microwave temperature for the activation to occur was found to be 150°C, and reinforced by the observation of PXRD data showed that there was no loss of crystallinity after the activation procedure (Fig. S10–S12, ESI†). The activation of DUT-84 resulted in a transition to a 'desolvated' phase which was observed by the original authors upon utilising their own activation procedure.[26] At higher temperatures (160-200°C), the MOFs were converted to an amorphous product, while at lower temperatures (120-140°C), a significantly reduced exchange efficiency was observed. The same was also true for increasing/ decreasing the duration of the activation in the microwave reactor, where 20 minutes at 150°C was found to offer the best exchange without degradation of crystallinity.

Thermal data was also obtained for each of the activated and non-activated samples (Figure 3). After the initial ramp, each sample was subjected to a 30-minute isotherm at 150°C to observe and ensure the complete removal of any adsorbed moisture and residual solvent, thus leaving only the SBU, the struts and any coordinated modulator. The post-isotherm mass loss was then noted for each sample (Table 2). nMOF-808 and aMOF-808 showed the greatest mass % loss after the second ramp. The large mass % loss for nMOF-808 can be attributed to the framework having the largest amount of bound acetate (Table 1). The second largest mass loss was observed for the DUT-84 variants. The UiO-66 variants showed the smallest reduction mass % after the second ramp, this is likely due to the framework having the smallest number of bound acetate per unit cell. Particularly interesting was the greater thermal stability of all activated MOFs after the second ramp (Figure 3). Unsurprisingly, MOF-808 showed the greatest mass % difference. This value can be ascribed to the activation process removing approximately 2.75 equivalents of acetate from each formula unit of the MOF (Table 1), and the largest quantity of the three MOFs. This was followed by DUT-84 and then UiO-66, respectively. The thermal mass % difference for each of the analysed MOFs was in agreement with the quantity of acetate removed, as determined by NMR.

Table 2. A comparison of the weight loss observed during TGA analysis for the non-activated and activated MOFs.

	nMOF-808	aMOF-808	nDUT-84	aDUT-84	nUiO-66	aUiO-66
Mass % Remaining[a]	88.3%	89.3%	93.0%	93.5%	92.9%	92.1%
Mass % Loss[b]	25.0%	16.2%	18.9%	12.3%	14.8%	9.3%
Rel. mass % Loss[c]	28.3%	18.1%	20.3%	13.2%	15.9%	10.1%
mass % Difference[d]		**10.2%**		**7.1%**		**5.8%**

[a]Mass % Remaining after maintaining a 150°C isotherm. [b]Mass % Loss after second ramp. [c]Relative mass % loss observed $(\frac{b}{a}) * 100$. [d]Difference in relative mass % Loss between the activated and non-activated materials.

After determining the degree of activation using NMR, and confirming the loss of modulator using TGA, we decided to investigate the hydrolytic capabilities of the activated MOFs and compare them to their non-activated counterparts.

Zirconium MOFs, particularly those with coordination defects, have been shown as highly effective hydrolysis catalysts for the degradation of V- and G-series nerve agents.[30,33] DMNP, buffered with an aqueous solution of N-ethyl morpholine, has been established as good simulant system for mimicking the hydrolysis of VX (diisopropyl-aminoethyl O-ethyl methylphosphonothioate) in solution, with good agreement in the degradation rates.

View Article Online
DOI: 10.1039/C7DT03616G

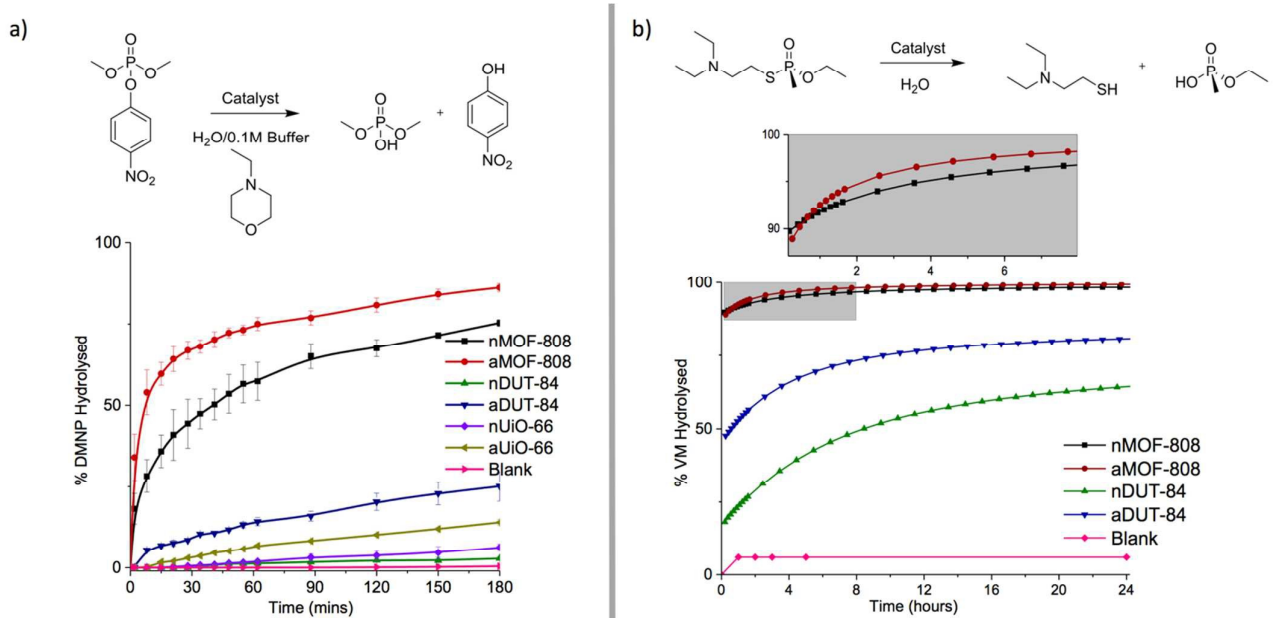

Figure 4. a) Reaction scheme for the hydrolysis of DMNP and a plot showing the hydrolysis of DMNP over time in the presence of the various MOF catalysts. Each set of data was obtained in triplicate and is shown with standard deviation error bars. **b)** Reaction scheme showing the selective hydrolysis of the agent VM along with a degradation plot showing the hydrolysis of VX over. Inset: highlights the slight difference between nMOF-808 and aMOF-808.

The buffered degradation of DMNP was found to best follow a first order rate model (Fig. S13 ESI†).

Figure 4a shows the results obtained for the hydrolysis study which was conducted with the activated and non-activated MOFs. aMOF-808 was the most effective degradation catalyst ($k = 9.5 \times 10^{-3}$ s^{-1}), closely followed by nMOF-808 ($k = 8.8 \times 10^{-3}$ s^{-1}). This can be explained by the 6-connected nature of aMOF-808 along with the 5.5 acetate-free coordination sites (Table 1). These catalytic sites are Lewis acidic and are able to facilitate the hydrolysis of the substrate in the presence of H_2O. nMOF-808 performed slower in the initial stage of the reaction but still performed relatively well compared to the other tested materials. This performance can be attributed to nMOF-808 framework possessing, on average, 2.75 vacancies per Zr_6 SBU. Both MOF-808 variants have a pore limiting diameter of ca. 10 Å which is the largest of all the MOFs investigated here, and large enough to facilitate the access of DMNP.

DUT-84 is a 6-connected framework and so we expected the hydrolysis rate to be somewhat similar to that of MOF-808. The degradation was however significantly slower, an explanation for this could be the 2D morphology of DUT-84. The two dimensionality results in less specificity for substrate access to hydrated nodes. Despite the degradation being rather slow, the degradation rate for aDUT-84 was significantly enhanced ($k = 1.8 \times 10^{-3}$ s^{-1}) over that of nDUT-84 ($k = 3 \times 10^{-4}$ s^{-1}), simply through the activation protocol. UiO-66 was the worst performer of the group. This was expected as aUiO-66 ($k = 1.2 \times 10^{-3}$ s^{-1}) has the smallest amount of acetate free sites compared to the other MOFs. As a control, we also synthesised UiO-66 using a modulator free procedure[14] and observed no discernible difference in reaction rate between pre-and post-microwave activation, and further demonstrates the utility of this modulator removal procedure.

The average pore limiting diameter in UiO-66 is ca. 5 Å,[34] which is smaller than the molecular size of DMNP. The catalytic activity is therefore restricted to just the surface of the framework, significantly reducing the number of accessible active sites.[35] Among the 3 MOFs tested, a general trend was observed where a higher pore limiting diameter correlated with a higher rate constant k for DMNP hydrolysis (Fig. S14–S15, ESI†). This correlation, comprising of only three data points, is tempered by the fact that the particle size for MOF-808 is much smaller than for DUT-84 resulting in much more accessible surface area for reactivity on the surface of MOF-808 (Fig. S16, ESI†).

After screening the three MOF catalysts with simulant DMNP, we chose to test MOF-808 and DUT-84 on the V-series agent VM, a diethyl analogue of VX, which was readily available at the time of testing. To further showcase the true applicability of the zirconium MOF-808 as a degradation catalyst, it was decided that the studies would be conducted in the absence of buffer. Excellent results were obtained for both nMOF-808 and aMOF-808 (Figure 4b). There was little discernible difference between the two catalysts because the first measurement could only be acquired 12 minutes after the reaction had commenced, at which point most of the VM had been hydrolysed. This was an unfortunate safety limitation of the experimental procedure. The first DUT-84 was also successful at hydrolysing VM, albeit, at a slower rate. As postulated, aDUT-84 significantly outperformed nDUT-84, and parallels with the simulant hydrolysis study. It should be noted that when the zirconium MOFs were used, only P-S bond cleavage of the VM occurred. This is highly desirable as the

View Article Online
DOI: 10.1039/C7DT03616G

hydrolysis product formed from P-O bond cleavage of a V-series agent results in a product which maintains its toxicity. For instance, hydrolysis with a strong base such as NaOH which results in the competitive cleavage of both P-O and P-S bonds. The above experiment further highlights the utility of these Zirconium MOFs for rapid and selective hydrolysis of V-series agents in the presence of only water (i.e. no buffer).

Conclusions

Three acetic acid modulated MOFs were activated using a highly facile method which relied on the use of microwave irradiation. Microwave irradiation enables instant, evenly distributed heating above boiling temperature, something which is difficult to achieve with an autoclave vessel. The extent of their activation was determined using NMR with MOF-808 showing the greatest degree of activation, while the enhanced thermal stability of each activated MOF, after removal of acetate modulator, was demonstrated using TGA. The activated MOFs, with hydrated nodes, were then employed in the catalytic hydrolysis of a CWA simulant and showed enhanced hydrolysis rates over that of their non-activated counterparts, and further shown to degrade VM without the necessity of a buffering reagent.

Acknowledgements

BAB and SJH are grateful to the Defence Science and Technology Laboratories for funding and Dr James T.A. Jones for facilitating the NMR analysis of the active V-agent. We would also like to thank the University of Kent for financial and in-kind support. The authors would also like to further acknowledge that YK is a DSTL-funded post-graduate researcher.

References

1 S. Yuan, Y. Chen, J. Qin, W. Lu, L. Zou, Q. Zhang, X. Wang, X. Sun and H. Zhou, *J. Am. Chem. Soc.* 2016, **138**, 8912-8919
2 A. M. Ploskonka and J. B. DeCoste, *ACS Appl. Mater. Interfaces,* 2017, **9**, 21579–21585.
3 J. B. DeCoste, G. W. Peterson, H. Jasuja, T. G. Glover, Y. Huang and K. S. Walton, *J. Mat. Chem. A.* 2013, **1**, 5642-5650.
4 F. Drache, V. Bon, I. Senkovska, C. Marschelke, A. Synytska and S. Kaskel, *Inorg. Chem.* 2016, **55**, 7206-7213.
5 X. Zhang, X. Zhang, J. A. Johnson, Y. Chen and J. Zhang, *J. Am. Chem. Soc.* 2016, **138**, 8380-8383.
6 H. Liu, Y. He, J. Jiao, D. Bai, D. Chen, R. Krishna and B. Chen, *Chem. Eur. J.* 2016, **22**, 14988-14997
7 J. Zhang, S. Yao, S. Liu, B. Liu, X. Sun, B. Zheng, G. Li, Y. Li, Q. Huo and Y. Liu, *Cryst. Growth Des.* 2017, **17**, 2131-2139.
8 H. Wang, Q. Wang, S. J. Teat, D. H. Olson and J. Li, *Cryst. Growth Des.* 2017, **17**, 2034-2040
9 M. H. Teplensky, M. Fantham, P. Li, T. C. Wang, J. P. Mehta, L. J. Young, P. Z. Moghadam, J. T. Hupp, O. K. Farha and C. F. Kaminski, *J. Am. Chem. Soc.,* 2017
10 I. A. Lázaro, S. Haddad, S. Sacca, C. Orellana-Tavra, D. Fairen-Jimenez and R. S. Forgan, *Chem,* 2017, **2**, 561-578
11 R. J. Marshall, Y. Kalinovskyy, S. L. Griffin, C. Wilson, B. A. Blight and R. S. Forgan, *J. Am. Chem. Soc.,* 2017, **139**, 6253-6260
12 F. Drache, V. Bon, I. Senkovska, M. Adam, A. Eychmüller and S. Kaskel, *Eur. J. Inorg. Chem.* 2016, **2016**, 4483-4489
13 E. Plessers, G. Fu, C. Y. X. Tan, D. E. De Vos and M. B. Roeffaers, *Catalysts,* 2016, **6**, 104.
14 M. Rimoldi, A. J. Howarth, M. R. DeStefano, L. Lin, S. Goswami, P. Li, J. T. Hupp and O. K. Farha, *ACS Catalysis,* 2016, **7**, 997-1014.
15 K. Užarević, T. C. Wang, S. Moon, A. M. Fidelli, J. T. Hupp, O. K. Farha and T. Friščić, *Chem. Commun.* 2016, **52**, 2133-2136
16 Y. Huang, W. Lo, Y. Kuo, W. Chen, C. Lin and F. Shieh, *Chemical Communications,* 2017, **53**, 5818-5821
17 S. Biswas and P. Van Der Voort, *Eur. J. Inorg. Chem.* 2013, **2013**, 2154-2160
18 M. Miyamoto, K. Hori, T. Goshima, N. Takaya, Y. Oumi and S. Uemiya, *Eur. J. Inorg. Chem.* 2017, **2017**, 2094-2099
19 C. Atzori, G. C. Shearer, L. Maschio, B. Civalleri, F. Bonino, C. Lamberti, S. Svelle, K. P. Lillerud and S. Bordiga, *J. Phys. Chem. C.* 2017, **121**, 9312-9324
20 R. J. Marshall, C. L. Hobday, C. F. Murphie, S. L. Griffin, C. A. Morrison, S. A. Moggach and R. S. Forgan, *J. Mat. Chem. A.* 2016, **4**, 6955-6963
21 G. C. Shearer, S. Chavan, S. Bordiga, S. Svelle, U. Olsbye and K. P. Lillerud, *Chem. Mater.* 2016, **28**, 3749-3761
22 J. Jiang, F. Gándara, Y. Zhang, K. Na, O. M. Yaghi and W. G. Klemperer, *J. Am. Chem. Soc.,* 2014, **136**, 12844-12847
23 L. T. Hoang, L. H. Ngo, H. L. Nguyen, H. T. Nguyen, C. K. Nguyen, B. T. Nguyen, Q. T. Ton, H. K. Nguyen, K. E. Cordova and T. Truong, *Chem. Commun.* 2015, **51**, 17132-17135
24 G. C. Shearer, S. Chavan, J. Ethiraj, J. G. Vitillo, S. Svelle, U. Olsbye, C. Lamberti, S. Bordiga and K. P. Lillerud, *Chem. Mater.* 2014, **26**, 4068-4071
25 E. López-Maya, C. Montoro, L. M. Rodríguez-Albelo, S. D. Aznar Cervantes, A. A. Lozano-Pérez, J. L. Cenís, E. Barea and J. A. Navarro, *Angew. Chem. Int. Ed.* 2015, **54**, 6790-6794
26 V. Bon, I. Senkovska, M. S. Weiss and S. Kaskel, *CrystEngComm,* 2013, **15**, 9572-9577
27 H. Furukawa, F. Gándara, Y. Zhang, J. Jiang, W. L. Queen, M. R. Hudson and O. M. Yaghi, *J. Am. Chem. Soc.,* 2014, **136**, 4369-4381
28 W. Liang, H. Chevreau, F. Ragon, P. D. Southon, V. K. Peterson and D. M. D'Alessandro, *CrystEngComm,* 2014, **16**, 6530-6533
29 S. Moon, Y. Liu, J. T. Hupp and O. K. Farha, *Angew. Chem. Int. Ed.* 2015, **54**, 6795-6799
30 J. E. Mondloch, M. J. Katz, W. C. Isley III, P. Ghosh, P. Liao, W. Bury, G. W. Wagner, M. G. Hall, J. B. DeCoste and G. W. Peterson, *Nature Mat.* 2015, **14**, 512-516
31 S. Moon, G. W. Wagner, J. E. Mondloch, G. W. Peterson, J. B. DeCoste, J. T. Hupp and O. K. Farha, *Inorg. Chem.,* 2015, **54**, 10829-10833
32 R. A. Moss, K. Alwis and G. O. Bizzigotti, *J. Am. Chem. Soc.,* 1983, **105**, 681-682
33 Y. Liu, S. Moon, J. T. Hupp and O. K. Farha, *ACS Nano,* 2015, **9**, 12358-12364.

View Article Online
DOI: 10.1039/C7DT03616G

34 M. J. Katz, Z. J. Brown, Y. J. Colón, P. W. Siu, K. A. Scheidt, R. Q. Snurr, J. T. Hupp and O. K. Farha, *Chem. Commun.* 2013, **49**, 9449-9451
35 A. J. Howarth, Y. Liu, P. Li, Z. Li, T. C. Wang, J. T. Hupp and O. K. Farha, *Nat. Rev. Mater.* 2016, **1**, 15018

Graphical Abstract: